

THE NOVELTIES IN THE DEVELOPMENT OF Na-ION BATTERIES

Slavko Mentus*

University of Belgrade, Faculty of Physical Chemistry, Studentski trg 12, 11000 Belgrade, Serbia
Serbian Academy of Sciences and Arts, Knez Mihajlova 35, 11000 Belgrade, Serbia

*Corresponding author: slavko@ffh.bg.ac.rs

Abstract: Today Li-ion batteries dominate as the power sources for portable electronics (mobile phones, lap-top calculators) as well as for electric cars. The main problem with their use is limited sustainability: the raw materials for their production: lithium, cobalt and nickel, are deficient in the earth's crust. Potential exhaustion of mining resources treats to disable the production of Li-ion batteries in near future. On the other hand, Na-ion batteries, which work on similar principles to Li-ion batteries, present a real sustainable alternative. Namely, the abundance of sodium in the earth's crust is far higher in comparison to lithium, and Na-ion batteries may be produced from very abundant metals, excluding cobalt and nickel. Thus, the development of Na-ion batteries is the subject of interest of a broad number of research groups worldwide. Currently, the main flaw of Na-ion batteries is lower energy density (~ 50 % that of Li-ion ones), thus the competitiveness in the market is still always relatively low, enabling the first generation of these batteries only complementary use in low-demanding areas, (for example in grid voltage stabilization). However, recently a number of improvements is realized, promising a rapid increase in the competitiveness of Na-ion batteries in all areas of use. In this work, the survey was made on the properties of commercial versions of first-generation batteries. Also, recent advances in improvements of anode and cathode materials which may lead to the second generation of Na-ion batteries are summarized.

Keywords: Na-ion batteries, cathode materials anode materials, commercial battery versions.

1. INTRODUCTION

After roughly three decades from their first commercialization (in 1990), the Li-ion batteries have taken over the battery market, thanks to their high practical energy density (actually~200 Wh/kg up to even 285 Wh/kg) and relatively low price, which during time descended from initial ~1500 US\$ per one kWh to actual ~ 150 US\$ per one kWh of energy. The high specific energy of lithium-ion batteries provides a long working time interval between charges, which is extremely important for the comfortable use of portable devices and electric cars. Thanks to its wide use in diverse kinds of portable electronic devices, as well as in electric cars, the demand for these batteries is permanently growing. Connected to the world trend of industry

decarbonisation, a new role of batteries arises in the area of storage and stabilization of the energy obtained from renewable sources. A French battery market forecast company, Avicenne Energy [1] forecasted the Li-ion battery market will attain more than \$150 billion by 2025., where the demand for energy storage systems alone is expected to amount to \$50 billion. The company Bloomberg New Energy Finance predicted that demand for lithium will experience an enormous 500-fold increase by 2030. That could cause lithium prices to expand because the metal is mined in only a few countries.

Accounting only for the production growth, one may expect that the cost of Li-ion batteries will proportionally decrease up to about \$100/kWh. However, on the other hand, production expansion

may cause the exhaustion of raw materials, primarily cobalt and nickel [2,3], which not only may increase the Li-ion battery price but hinder their production at all.

This is why more than a decade ago scientists searched for a sustainable alternative for Li-ion batteries, focusing primarily on Na-ion batteries. The advantage of Na-ion batteries lies in higher natural abundance and lower cost of sodium in comparison to lithium. Namely, 2.6% of sodium can be found in the earth's crust, compared with barely 0.06% of lithium. The cost of extraction of Na of only \$150 ton^{-1} is much lower than that of Li, being \$5000 ton^{-1} [4] Moreover, cathode materials for Na-ion batteries do not require cobalt and nickel, and contain abundant, and also environmentally benign transition metals, such as iron, manganese, vanadium, and titanium. Thus, Na-ion batteries with hard-carbon anodes and cobalt-free cathodes are more sustainable than Li-ion batteries. Since the cost of production of the electrode materials for Li-ion and Na-ion batteries is almost equal the gain in costs of Na-ion batteries originates in the price of raw materials only. The survey of actual prices of raw materials allows us to conclude the cost of Na-ion batteries to be 10–20% lower than the Li-ion ones, and this difference is concentrated mainly in the costs of cathode materials. Sodium batteries are also more stable and safer than lithium-ion ones. They may withstand a wider temperature range, are less flammable and less prone to thermal runaway—contrary to the main flaws of Li-ion batteries [4.] According to K. M. Abraham, research professor at Northeastern University and CTO of lithium battery consulting firm E-KEM Sciences, the main disadvantage of Na-ion batteries which suppresses their competitiveness is lower energy density, attaining up to now $\sim 100 \text{ Wh kg}^{-1}$ or in best cases $\sim 150 \text{ Wh kg}^{-1}$. This is why sodium-ion batteries presently could find application only in stationary applications like renewable energy storage for homes and the grid energy stabilization, where cost is more important than size and energy density. Therefore, to reach full competitiveness, the researchers should focus their care on advanced anode and cathode materials which enable specific energies approaching at least 200 Wh kg^{-1} . This may require also the search for advanced electrolytes.

Theoretical considerations by Slater et al. [5] indicate that sodium-ion battery may attain gravimetric energy density of 210 Wh kg^{-1} , fully

comparable to the energy density of actual Li-ion batteries, if cathode specific capacity of 200 mAh g^{-1} and anode specific capacity of 500 mAh g^{-1} , with an average potential difference of 3.3 V may be discovered. The voltage between anode and cathode is an essential value since the energy density is the product of the specific capacity of cathode (or anode) material and voltage. This statement may be used as a guide in the further development of sodium-ion batteries. However, not capacity value alone, but also its stability upon numerous charging/discharging cycles, as well as low sensitivity to high charging/discharging rates present an indispensable characteristic providing their use in most important application areas.

In this review, a survey of recent research reports on substantial components of sodium-ion batteries is done. This survey shows that recently discovered anode and cathode materials are sufficiently close to those enabling actual competitiveness to contemporary lithium-ion batteries, which supports the promises of leading battery producers that their next generation of sodium-ion batteries will serve as a satisfactory supplement or even replacement for lithium-ion batteries.

2. ANODE MATERIALS OF Na-ION BATTERIES

2.1. Hard carbon anode materials

Sodium-ion batteries became to attract attention about a decade after the commercialization of Li-ion batteries. Natural or synthetic graphite is a common anode material for these batteries, however, the attempts to use graphite as anode material also in Na-ion batteries were unsuccessful. Namely, Ge et al [6] found the low initial capacity of graphite in the usual ethylene carbonate-ethyl-methyl carbonate mixture, of roughly 30 mAh g^{-1} , together with poor cycle life, since initial capacity dropped to even negligible value within the few charging/discharging cycles. The first explanation was that the interlayer distance between graphite crystallographic planes ($\sim 3.3 \text{ nm}$) is too small to enable Na^+ ions diffusion through the graphite bulk. Further to this, Divincenzo et al. [7] found theoretically that the attractive forces between the Na^+ ions and the graphite layers are too low to support the

intercalation, and thus unwanted plating of carbon surface by metallic sodium occurs more readily than intercalation.

Dahn et al [8] were among the first ones to discover the applicability of hard carbons as the anode of sodium-ion batteries. They pyrolyzed glucose at 1000 °C and examined its anode behavior in a solution of 1 M sodium perchlorate in ethylene carbonate – diethyl carbonate (30:70 v/v mixture) and found a reversible capacity of ~ 300 mAh g⁻¹ at a very slow charging-discharging rate C/80 (35 μA/cm²).

Hard carbons are a particular kind of carbon, composed of statistically oriented micron-sized graphite domains leaving many intercrystalline pores of various dimensions. (Figure 1). Hard carbons may be synthesized from various natural precursors, for instance, glucose, sucrose, lignin, cellulose, various organic polymers etc. The precursor should contain a high concentration of oxygen. Namely, the remaining oxygenated groups enable to keep disordered structure upon carbonization, i.e., randomly-oriented graphitic domains and larger mean interlayer spacing (~0,39 nm), providing easy diffusion of sodium as well as the acceptable capacity of sodium storage. This type of carbon is not able to transform itself into crystallographically ordered graphite by heating up to even 3000 °C, thus it is called alternatively non-graphitizable carbon.

In 2011, Wenzel and co-works [9] prepared templated carbon with controlled hierarchical porosity, with a surface area of 346 m² g⁻¹, and pore volume of 0.798 cm³ g⁻¹. They published a high capacity of 100 mAh g⁻¹ at an excellent charging/discharging rate of C/5, much higher than C/80 attained in early attempts by Dahn et al [8] at room temperature. Their results indicated that, if

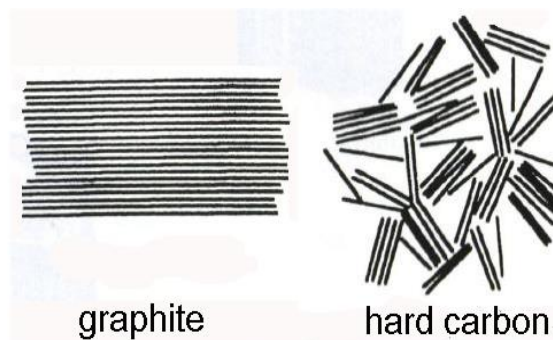


Figure 1. Structure difference between graphite and hard carbon: long-range versus short-range ordering of graphene layers.

hard carbon is considered, a high specific surface is not a critical factor in obtaining high capacity and rate capabilities. Somewhat later, in 2014., Zhou et al [10] obtained structurally disordered carbon by pyrolysis at 800 °C of an intimate mixture of soluble polymers poly(diallyl dimethylammonium chloride) (PDDA) and poly(sodium 4-styrenesulfonate) (PSS), and the average spacing between the graphitic layers of 0.39 nm was determined. When used as anode material in the electrolyte 1M NaClO₄ (1M) in solvent mixture propylene carbonate + ethylene carbonate, superior capacity, cycling stability and rate capability were evidenced. A reversible capacity of 225 mAh g⁻¹ was attained, while capacity retention of 92% at a current density of 100 mA g⁻¹ was achieved after 180 cycles.

Typical galvanostatic charging and discharging curves of hard carbon in organic solution of sodium salt are shown in Figure 2. On charging (sodiation), initial part of charging curve shows sudden potential drop to below 1 V, as a consequence of the incorporation of first traces of sodium. Then follows a sloped part of the curve, which covers a great part of charge consumed. This part continues to a plateau close to 0 V, which covers also a significant part of the charge consumed. First charging (curve 1) consumes more electricity than the following ones (curves 2 and 3), due to the formation of a solid electrolyte interface (SEI), which is analogous to the behavior of graphite in Li-salt solution. The desodiation curve, with its high-voltage end, shows the amount of reversibly intercalated sodium ions. Usually, a stable regime (overlapping of successive

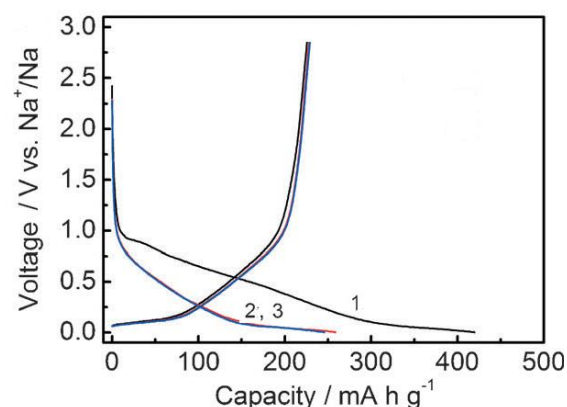


Figure 2. Galvanostatic sodiation (descending V) and desodiation (ascending V) curves of hard carbon electrode in organic solution of sodium salt

discharging curves) may be attained in a few initial charging/discharging cycles.

The mechanism of charging/discharging processes shown in Figure 2 was studied theoretically by several authors. Tsai et al. [11], through an *ab initio* study found that not only interlayer distance but also the concentration of vacancy defects (MV: mono-vacancy and DV: di-vacancy) improve the Na⁺ ion intercalation. Namely, vacant sites enable strong ionic binding with the Na⁺ ions, which overcomes the van der Waals interaction. Bommier et al. [12] stated that the sloping region of the charging curve can be explained through Na⁺ ion storage at defect sites. In the plateau region, they confirmed that Na⁺ ions intercalate into a lattice of crystallites. Rathnayake et al [13] found by DFT calculations that an interlayer distance of ~6 nm provides optimum interaction energy for sodium intercalation.

As Hwang reviewed in [14] the electrochemical behavior of hard carbons may be substantially improved by the incorporation of heteroatoms (such as N, B, S and P) by any doping procedures. Namely the sites containing the atoms of dopants enhance the adsorption of Na⁺ ions and facilitate the transport of sodium ions through the electrode-electrolyte boundary.

For instance, Wang et al. [15] synthesized N-doped hard carbon by carbonization of pulp obtained from milled soybeans. The samples presented flexible films composed of nitrogen-doped porous nanofibers with a 3D interconnected structure. The capacity of 212 mA h g⁻¹ at a high rate of 5 A g⁻¹ with high-capacity retention of 99% after even 7000 charging/discharging cycles were attained. Sulphur doping provided even better results. In 2015, Li et al. [16] synthesized a disordered carbon doped with sulfur with a high doping level (~26.9%), by annealing at 500 °C in an argon flow the mixture of 1,4,5,8-naphthalene tetracarboxylic dianhydride (NTCDA) and sulphur.

This material displayed a specific 3D coral-like structure. This carbon type exhibited a high reversible capacity of 516 mAh g⁻¹ at a current density of 0.02 A g⁻¹. Also, an excellent rate capability and cyclability, 271 mAh g⁻¹ at 1 A g⁻¹ after 1000 cycles, was reported. This result may enable almost full competitiveness of Na-ion batteries to Li-ion ones in practical application.

Li et al [17] synthesized hard carbon-doped by nitrogen, which was additionally modified by doping of phosphorus quantum dots. The raw

materials were soybean pulp, the carbonization of which resulted in N-doped carbon. Then, the mixture of red phosphorus and water was heated in a hydrothermal reactor. Upon precipitate removal, the solution containing P quantum dots was concentrated by centrifuge and mixed with N-doped carbon. The solvent was removed by drying, and the resulting double-doped carbon (designated as P/NC) was tested electrochemically. This material displayed a stable capacity of 220 mAh g⁻¹ at a current rate of 0.3 A g⁻¹ during 5000 charging/discharging cycles. Also, a full cell consisting of Na_{0.58}Ni_{0.33}Mn_{0.67}O₂ cathode (in excess) and P/NC anode was tested and delivered a capacity of 150 mAh g⁻¹ at a rate of 1C, and 52 mAh g⁻¹ at a very high current rate of 30 C.

2.2. Expanded graphite anode

Since graphite was proven to be unsuitable for sodium-ion batteries having a very low capacity, researchers started to search for materials more suitable for this purpose. Suspecting too short interlayer spacing of regular graphite as a reason for low capacity, Wen et al [18] reported expanded graphite as a Na-ion battery anode material. The synthesis consisted of a multiplied process of oxidation and partial reduction of graphite until a relatively large interlayer distance of 0.43 nm was achieved. Galvanostatic studies in sodium salt solutions in organic solvents demonstrated that graphite with such expanded interlayer distance delivered a reversible capacity of 284 mAh g⁻¹ at a current rate of 20 mA g⁻¹, while a capacity of 184 mAh g⁻¹ was observed at the current rate of 100 mA g⁻¹. Also, a very good cycle life was demonstrated, namely, 73.92% of the initial capacity value was measured after 2,000 charging/discharging cycles.

2.3. Graphene oxide-based anode materials

The attempts to use graphene as anode material are known from earlier. Wang et al. [19] investigated sodium-ion storage using reduced graphene oxide (RGO) as anode material and found promising reversible electrochemical behaviour. This was explained by high electrical conductivity, large interlayer distances and the presence of numerous active sites for binding Na⁺ ions. Specific capacity of 141 mAh g⁻¹ at 40 mA g⁻¹ and stable capacity retention during 1000

charging/discharging cycles were reported. Ding et al. [20] synthesized several versions of few-layer graphene at carbonization temperatures in a broad temperature range of 600–1400 °C. They found promising Na⁺ insertion performances of graphene obtained at 1100 °C, having an enlarged interlayer spacing of 0.388 nm.

Dobrota et al [21] performed a DFT study of Na interaction with graphene sheets doped by heteroatom dopants (B, N, P or S), in both oxidized and non-oxidized stages. The calculation of interaction energy displayed that oxidation plays a crucial role in the interaction with sodium atoms. It was found that the dopants act as attractors of OH groups, and expand the ability of graphene to further oxidation altering also its affinity towards Na. Since in some specific cases this may lead to irreversible hydroxide or water formation, this may mean irreversible electrode performance degradation. These results suggested that carefully control of the oxidation level of doped graphene is required, depending on its dopant nature, to provide optimal performance in sodium storage processes.

Graphene alone did not enable high specific capacitances for Na ion storage, however, its composite with other materials having very high coulombic capacities, such as SnS₂, MoS₂, and phosphorus (for instance in phosphorene form) present very promising anode materials. These materials show high capacities of the order of thousands of mAh g⁻¹, however, extreme volume expansion and low electric conductivity hinder their direct use in batteries. The volume expansion is the consequence of the “alloying” reaction with sodium, and the swelling may amount to more than 400 to 500 per cent of the initial volume when the battery is charged, which may cause mechanical damage and loss of electrical contact with the current collector. The composite with graphene provides a synergetic effect of high electric conductivity, high capacity, and acceptably mitigated volume changes during the charging/discharging procedure.

2.3.1. Graphene/MoS₂ composite anodes

David et al. [22] from the research group at Kansas State University, discovered that some transition metal dichalcogenides may be exfoliated in strong acids. For the last two years, they developed the synthesis of large quantities of two-dimensional materials — graphene, molybdenum

and tungsten disulphide. They have published paper-like material composed of two 2D materials: molybdenum disulphide and graphene, which overcomes the shortcomings of both materials. For the synthesis, they used acid-exfoliated few-layer molybdenum disulphide (MoS₂) and reduced graphene oxide (rGO). Both components were dispersed in deionized water in various weight ratios and deposited by filtration, resulting in self-standing flexible electrode material (Figure 3). This design enables it to work without the polymeric binder and current collector foil, used traditionally in battery electrodes. The porous and interleaved structure of this electrode material enables fast sodium diffusion, and consequently, fast charging and discharging of the battery. The authors studied the electrochemical performance of this material in sodium-ion batteries. In a configuration with a metallic Na counter electrode the composite paper anode with the loading of 4 mg cm⁻² displayed a stable coulombic capacity of approximately 230 mAh g⁻¹ and coulombic efficiency of roughly 99%.

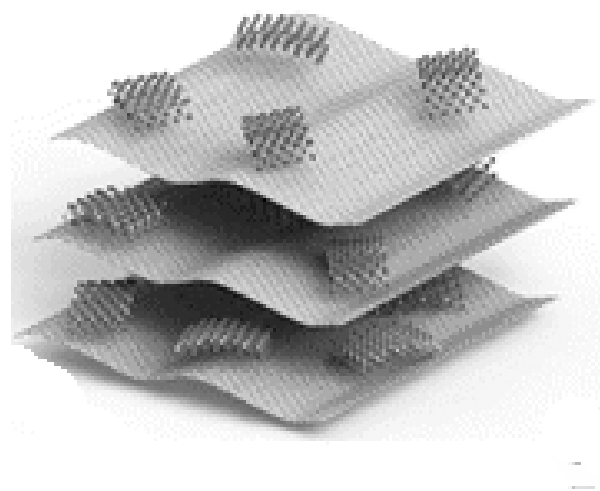


Figure 3. Scheme of the composite of layered MoS₂ crystals sandwiched between graphene oxide layers [22] Copyright ACS (2014)

Pan et al [23] considered an alternative way of the use of MoS₂ as anode material in sodium-ion batteries (SIBs). To minimize irreversible conversion reactions and huge volume changes accompanying the sodiation/desodiation reactions, the authors incorporated MoS₂ particles within carbon microtubes. This composite enabled fast electronic and Na⁺ ions conductivity, and low volume change during the sodiation/desodiation

reactions. A high reversible specific capacity of $563.5 \text{ mA h g}^{-1}$ at the current rate of 0.2 A g^{-1} , and even $401.3 \text{ mA h g}^{-1}$ at the current rate of 10.0 A g^{-1} , were achieved. Also, excellent cycling stability of $484.9 \text{ mA h g}^{-1}$ after 1500 cycles at the current rate of 2.0 A g^{-1} was evidenced.

2.3.2. Graphene/SnS₂ composite anode

Thanks to its huge specific capacity, SnS₂ has been extensively studied as an anode material for sodium storage. However, irreversible conversion/restacking reactions during the charge/discharge process rapidly lower the coulombic efficiency (ICE) Jiang et al [24] reported a one-step hydrothermal synthesis of graphene/SnS₂ composite with ultrathin SnS₂ nanosheets covered by neighborhood attached reduced graphene oxide layers, where C–S bonds provide mechanical stability. The composite interlayer spacing of SnS₂ layers was 0.803 nm , which enables fast transport of Na⁺ ions whereas restacking reactions of SnS₂ nanosheets were inhibited. An excellent specific capacity of 765 mAh g^{-1} for sodiation/desodiation reactions at a high rate of even 10 A g^{-1} was evidenced. No morphology changes were evidenced after 200 cycles. The authors stated they found an excellent anode material for sodium batteries.

Ou et al [25] considered a different type of composite to utilize layered SnS₂ as anode material of sodium-ion batteries. They synthesized SnS₂/Mn₂SnS₄ composite incorporated between carbon nano boxes by a wet-chemical method. This anode material displayed an initial capacity of 841.2 mAh g^{-1} with high coulombic efficiency of 90.8%. The rate performance examination evidenced capacities of 752.3 and 488.7 mAh g^{-1} at the current rate of 0.1 , and 10.0 A g^{-1} , respectively. Pronounced cycling stability was evidenced by measuring 522.5 mAh g^{-1} after 500 charging/discharging cycles at the current rate of 5.0 A g^{-1} . The coarsening of reaction products Sn and Na₂S are prevented thanks to the SnS₂/Mn₂SnS₄ heterojunctions, which play a key role in preventing capacity fade during cycling. These heterostructures together with the carbon network provide transparent ways for electrons and Na⁺ diffusion, resulting in an excellent rate performance.

2.3.3. Graphene/phosphorene layered anode materials

Black phosphorus is an allotropic modification of phosphorus. It has a layered structure, the layers presenting a two-dimensional material consisting of phosphorus atoms interconnected in a zig-zag order (Figure 4) may be separated either mechanically, or chemically, and separated layers are called phosphorene. Likely to graphene, the Van der Waals forces held the layers together in black phosphorus crystals. Phosphorene is a new material, namely, it was first produced in 2014 by mechanical exfoliation.

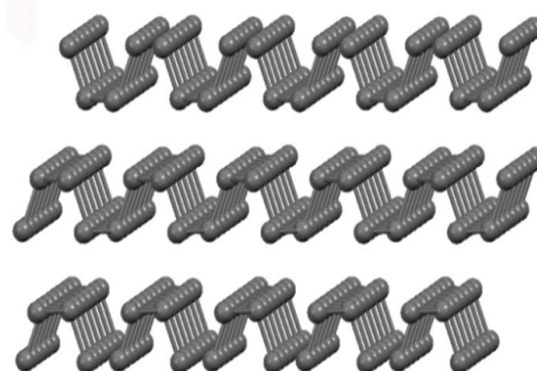


Figure 4. Scheme of the layered crystallographic structure of black phosphorus

Ramireddy et al. [26] studied composite electrode material composed of a mixture of black phosphorus with graphite. They prepared the composite by ball milling. Electrochemical testing was performed within different voltage windows. Within the voltage window of $0.01\text{--}2 \text{ V}$ versus the Na/Na⁺ electrode, a high initial capacity of 1300 mAh g^{-1} was obtained, however, the capacity displayed a gradual decrease, and the electrode material disintegrated on cycling. Much better behavior was observed within a restricted voltage window of $0.33\text{--}2.0 \text{ V}$ when repeated cyclic voltammograms indicated stable behavior. Sun et al. [27] synthesized a phosphorene–graphene hybrid composite, consisting of a few phosphorene layers sandwiched between graphene layers. The nanocomposite material displayed the following advantages: The graphene layers acted as a buffer mitigating volume expansion to which phosphorene layers are prone to sodiation, and provide high electronic conductivity of this electrode material as well. Furthermore, the

increased interlayer distance between phosphorene layers facilitates the diffusion of sodium ions. In electrochemical tests, this material displayed high coulombic capacity being stable on sodiation/desodiation cycling. As a result, this composite material provided a huge specific capacity of 2440 mAh g⁻¹ at a charging rate of 0.05 A g⁻¹. Upon 100 cycles within the voltage range of 0–1.5 V vs. Na/Na⁺, capacity retention of 83% was observed, which is a very promising result from the aspect of the development of Na-ion batteries.

2.4. Organic anode materials

Abouimrane et al. [28] discovered that disodium terephthalate-based organic material may be used as effective anode material of sodium-ion batteries, in combination with any transition-metal cathode. Since Na₄C₈H₂O₆ electrode displayed two reversible redox reactions, Na₂C₈H₂O₆/Na₄C₈H₂O₆ at 2.3 V and Na₄C₈H₂O₆/Na₆C₈H₂O₆ at 0.3 V (Figure 5). Wang et al. [29] fabricated a full cell with Na₄C₈H₂O₆ as both anode and cathode. This battery displayed a working voltage of roughly 1.8 V and reversible capacity of 180 mA h g⁻¹.

Deng et al [30] reported also an all-organic Na-ion battery with polymeric electrodes. The cathode was p-dopable polytriphenylamine and the

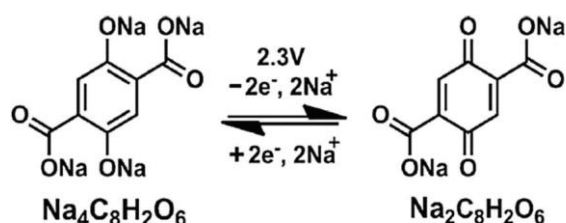


Figure 5. The scheme of the oxido/reduction reactions of solid Na₄C₈H₂O₆ in a solution of sodium salt.

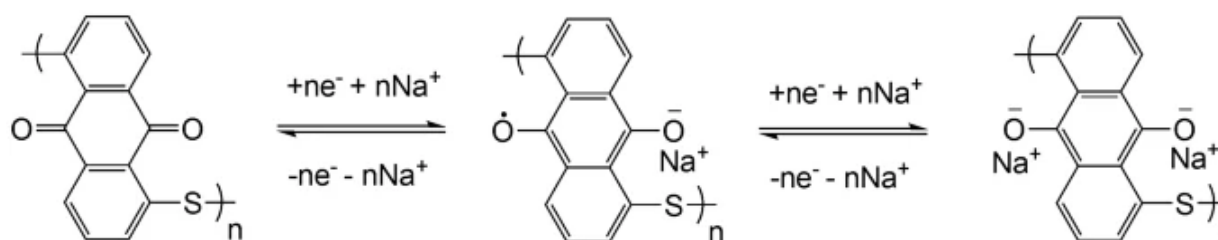


Figure 6. Proposed mechanism of poly(anthraquinonyl sulphide) redox reactions with participation of Na-cations. From Deng et al [30]

anode was an n-type redox-active poly(anthraquinonyl sulphide), in a solution of NaPF₆. The cathode was not a Na hosting material, but hosted concomitant PF₆⁻ anions, while the anode served as a host for Na⁺ insertion (Figure 6). Such battery delivered a voltage output of 1.8 V and specific energy of 92 Wh kg⁻¹. A superior rate capability was also evidenced, namely 60% of initial capacity was obtained at a very high rate of 16 C (3200 mA g⁻¹). Also, 85% capacity retention after 500 cycles at the current rate of 8 C was reported.

Chi et al [31] reported the organic carbonyl compound disodium rhodizonate (Na₄C₆O₆) with an average voltage of 2.15 V versus Na⁺/Na and a theoretical specific capacity of 205 mAh g⁻¹, which may be attained by two-electron and two-sodium ion exchange between reduced (Na₄C₆O₆) and oxidized (Na₂C₆O₆) forms of this compound. A practically attained capacity of 184 mAh g⁻¹ with metallic sodium anode was attained presenting high specific energy of 395 Wh kg⁻¹. The capacity retention of 76% and 70% was evidenced after 100 cycles at 0.1C and 400 cycles at 0.2 C, respectively. This compound was compatible with solid electrolyte Na₃PS₄, the authors constructed a symmetric all-organic cell Na₄C₆O₆/Na₃PS₄/Na₄C₆O₆ with solid electrolyte, which displayed an initial capacity of ~160 mAh g⁻¹ and 100 % efficiency at a rate of 0.2 C at 60 °C, while the capacity of ~125 mAh g⁻¹ was measured after 50 cycles.

2.5. Anode-free Na-ion battery

In a very recent paper, Ma et al [32] investigated how to prepare an anode-free battery version, in which pure metallic sodium anode grows on copper support just on battery charging, and dissolves on discharging. Batteries with metallic anodes are advantageous since they enable high energy density, but such type anodes usually experienced difficulties caused by dendritic growth

and formation of solid-electrolyte interphase (SEI) layers, which both shorten battery cycle life. Ma et al solved this problem by the discovery that high purification of electrolytes from water traces enables the formation of smooth, dendrite-free sodium surface, lacking in SEI formation on sodium deposit, thus having a large cycling life.

In their experiments, Ma et al used as cathode material $\text{Na}_3\text{V}_2(\text{PO}_4)_3$ (NVP) synthesized by hydrothermal sol-gel procedure and calcined at 750 °C for 6 h. It was mixed with acetylene black and polyvinylidene fluoride glue in a mass ratio of 8:1:1, and suspended in N-methyl pyrrolidone. This slurry was applied on Al foil support at loading 6.2 mg cm⁻². Anode support was Cu (25-micron foil), and the separator was porous Polypropylene. It is desirable to achieve water content lower than 10 ppm. The NaPF₆-based electrolytes were built up with organic solvents: dimethylethylene oxide, diglyme, tetraglyme, or ethylene carbonate/dimethyl carbonate mixture. The moisture level was in the range of 5-10 ppm in that case. Also, the NaClO₄-based electrolytes were tested with the same solvents, with the moisture level allowed in the range of 28-35 ppm, due to an extreme hygroscopicity of NaClO₄.

The full cell of anode-free type with low content of impurities in electrolyte displayed an excellent capacity retention rate of 99.93% per cycle, superior to available anode-free Na and Li batteries using liquid electrolytes. The gravimetric energy density (334.7 Wh kg⁻¹ at a very high current rate of 3C) of these anode-free cells was found to be comparable to the theoretical energy densities of Graphite|LiFePO₄ battery of 385 Wh kg⁻¹. Furthermore, this cell is smaller in volume because of the absence of an anode. The abundant resources of sodium in the earth's crust and the avoidance of anode processing costs make this type of cell more sustainable and economic in comparison to contemporary Li-ion cells.

3. CONTEMPORARY INVESTIGATIONS OF CATHODE MATERIALS

3.1. Layered oxides cathode materials

Analogously to the layered oxide materials used in contemporary Li-ion batteries, $(\text{LiCo}_{0.33}\text{Ni}_{0.33}\text{Mn}_{0.33}\text{O}_2, \text{LiCo}_{0.15}\text{Ni}_{0.8}\text{Al}_{0.05}\text{O}_2)$

layered oxides may be used also for Na ion intercalation. The layered oxides as cathodes for Na-ion batteries (SIBs) commonly appear as O3-phase and P2-phase. The O3 phase is characteristic of alternate Na layers and transition-metal (M) layers in the oxygen-ion framework, packed closely to form alternate ABCABC stacks. The symbol O3 means that the Na⁺ ions and M ions are located in the octahedral sites of the Na layers and the M layers. In the P2 phases, the oxygen-ion framework of the P2-phase is stacked in the ABBAABBA order. The Na⁺ ions are placed in the trigonal prismatic sites of the Na layers. Na⁺ ions can be reversibly inserted and deinserted between the (MO₂)_n sheets formed by edge-shared MO₆ octahedra.

Both these phases may be synthesized in the air by some common synthesis procedures: solid-state reactions, co-precipitation, or hydrothermal ones. O3-Na_xMnO₂ exhibits a capacity of 185 mAh g⁻¹ at 0.1 C in the potential range of 2.0–3.8 V and retains 132 mAh g⁻¹ after 20 cycles [33]. Birnessite-NaMn₃O₅ reveals a particularly large discharge capacity of 219 mAh g⁻¹ in the potential range of 1.5–4.7 V with an average potential of 2.75 V, but only 70% of the capacity is retained after 20 cycles [34].

The main obstacle to the practical use of these materials is the fast capacity fade during cycling. This problem was reduced significantly by partial replacement of Mn for Ni. The P2 compound Na_{0.67}Ni_{0.33}Mn_{0.67}O₂ was first reported in 2001 [35]. This compound displayed a capacity of roughly 165 mAh g⁻¹ and a higher potential of over 4V versus the sodium metal reference electrode. The potential increase was attributed to the participation of the Ni³⁺/Ni⁴⁺ redox couple. In a very recent paper, Zhang et al [36] proved that the capacity at the 4.2 V plateau is contributed to the irreversible O²⁻/O₂ⁿ⁻/O₂ evolution. Oxygen release and subsequent surface lattice densification were found to be responsible for the largely irreversible capacity loss during the initial cycle. In the same study, the authors found that the oxygen release may be suppressed by partial Fe substitution. Namely, the formation of Fe-(O-O) species, provides reversible O²⁻/O₂ⁿ⁻ redox reactions at high operating voltage. This means, that a more pronounced covalency of the TM-O bond may suppress the oxygen release in this type of compound, which improves also the electrochemical performance.

Kim et al [37] developed cathode material with the formula Na(Li_{1/3}Mn_{2/3})O₂ for which an

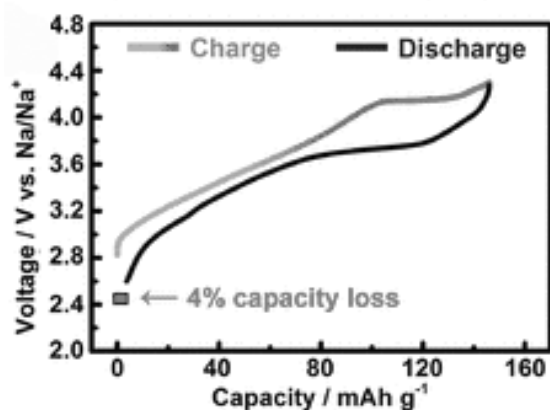


Figure 7. Charge/discharge curve of $\text{Na}_{2/3}\text{Fe}_{2/9}\text{Ni}_{2/9}\text{Mn}_{5/9}\text{O}_2$ in organic electrolyte solution of sodium salt [36]

appreciable specific capacity of 190 mAh g^{-1} was predicted theoretically. It is noteworthy that in this case sodium cation intercalation/deintercalation is accompanied not by $\text{Mn}^{4+}/\text{Mn}^{3+}$ redox reaction but by anionic redox reaction ($\text{O}^{2-}/\text{O}_2^{n-}$), at high redox potentials of $\approx 4.2 \text{ V}$ vs Na/Na^+ electrode. This means that, in this compound transition, the metal cationic state (Mn^{4+}) is stabilized.

The characteristics of this mixed oxide were studied experimentally by the researchers of Skoltech, a Russian private international university established in collaboration with the Massachusetts Institute of Technology (MIT). They cooperated with the researchers from France, the US, Switzerland, and Australia, [38] They confirmed that this cathode material displayed the reversible specific capacity of 190 mAh g^{-1} , which is rather high for a cathode material of sodium-ion batteries. Also, appreciable capacity retention was observed during prolonged cycling of $\text{Na}(\text{Li}_{1/3}\text{Mn}_{2/3})\text{O}_2$. The negligible sensitivity to moisture is also an important advantage of this material in comparison to LiMnO_2 . However, large voltage hysteresis during charge and discharge, causing a decrease in the energy efficiency, remains an actual obstacle in practical application, which is a challenge for further consideration. This study enabled new knowledge about the role of inter- and intralayer 3D cationic migration in the explanation of voltage fade in anionic redox materials.

3.2. Mixed phosphate cathodes

Mixed phosphates are composed of phosphate $(\text{PO}_4)^{3-}$ and pyrophosphate $(\text{P}_2\text{O}_7)^{4-}$

anions and belong to the polyanion class of materials. The class of materials $\text{Na}_4\text{M}_3(\text{PO}_4)_2\text{P}_2\text{O}_7$ (M: Mn, Co, Ni) was discovered in 1990-ties by Sanz et al. [39]. The structure of these compounds makes corners share MO_6 octahedra and PO_4 tetrahedra. $\text{M}_3\text{P}_2\text{O}_{13}$ blocks parallel to the bc plane are linked with the P_2O_7 unit along the a -axis. One distinguishes four different Na^+ sites in this structure, which are located in the three-dimensional channels. A free diffusion within all three dimensions provides better Na^+ ion conductivity in comparison with 2D or 1 D diffusion counterparts. Based on the first principal calculations, Kim et al. [40] for $\text{Na}_4\text{Fe}_3(\text{PO}_4)_2\text{P}_2\text{O}_7$ found a low activation barrier of less than 0.8 eV for Na^+ diffusion in all directions, with the lowest activation barrier in the large tunnel along the b -axis. The principal factor suppressing high specific capacities attainable in conventional Li-ion materials is the high molecular weight. In the experimental part of the study, $\text{Na}_4\text{Fe}_3(\text{PO}_4)_2\text{P}_2\text{O}_7$ synthesized by the usual solid-state reaction displayed a specific capacity of 105 mAh g^{-1} at an operating voltage of 3.2 V and an energy density of 380 Wh kg^{-1} . During charging $\text{Na}_4\text{Fe}_3(\text{PO}_4)_2\text{P}_2\text{O}_7$ to $\text{Na}_4\text{Fe}_3(\text{PO}_4)_2\text{P}_2\text{O}_7$ three sodium ions may be extracted, based on the redox reactions of the $\text{Fe}^{2+}/\text{Fe}^{3+}$ redox couple. [41] Instead of Fe containing central ion, to obtain higher operation potential Nose et al. [42] investigated $\text{Na}_4\text{Co}_3(\text{PO}_4)_2$. Indeed, they found an average operating voltage of approximately 4.5 V , being the highest value ever observed for a Na-ion electrode. The material displayed promising rate behavior, namely capacity of 80 mAh g^{-1} was measured at a current rate of even 25C , or 4.25 A g^{-1} . To flatten the stepped charging/discharging voltage curve, they synthesized $\text{Na}_4[\text{Co}_{2.4}\text{Mn}_{0.3}\text{Ni}_{0.3}](\text{PO}_4)_2\text{P}_2\text{O}_7$. Which displayed also a high operating voltage of 4.5 V , and delivered a discharge capacity of 103 mAh g^{-1} at a current rate of 5C .

Another interesting phosphate polyanion compound, $\text{Na}_7\text{V}_4(\text{P}_2\text{O}_7)\text{PO}_4$, was suggested by Lim et al. [43]. This compound crystallized in a tetragonal structure, with the basic unit, $(\text{VP}_2\text{O}_7)_4\text{PO}_4$, composed of a central tetrahedron $[\text{PO}_4]$ sharing corners with four $[\text{VO}_6]$ octahedral. Each diphosphate group $[\text{P}_2\text{O}_7]$ bridges the two adjacent $[\text{VO}_6]$ octahedral with shared corners. The three-dimensional diffusion of Na ions is possible, through channels formed by interconnected $(\text{VP}_2\text{O}_7)_4\text{PO}_4$ units. The charging/discharging process is accompanied by a $\text{V}^{3+}/\text{V}^{4+}$ redox reaction,

which occurs at an average voltage of 3.9 V delivering a capacity of approximately 90 mAh g⁻¹. Forming a composite material with reduced graphene oxide, cycle life was improved providing 78 % capacity retention after 1000 cycles.

Particularly high voltages may be obtained with sodium vanadium fluorophosphates. Yuvaraj et al [44] reviewed this group of compounds. Among the fluorophosphate groups, Na₃V₂(PO₄)₂F₃ exhibited the highest theoretical capacity (128 mAh g⁻¹) and working voltage (~3.9 V vs. Na/Na⁺) compared to the other fluorophosphates. For this compound, Zhao et al [45] found a specific capacity of 101 mAh g⁻¹ at a very high current rate of 30C after even 3500 cycles, and 75 mAh g⁻¹ at a still higher current rate of 70 C.

Many recently published studies involving mixed phosphate cathode material were the subject of a review by Gezovic et al [46] This review is focused on the development of a family of isostructural polyanion phases encompassed by the common chemical formula Na₄M₃(PO₄)₂P₂O₇, where M is Fe, Ni, Co and Mn. A comprehensive retrospective of their synthesis procedures, the kinetics and the mechanism of sodiation/desodiation reactions is provided. Structural properties were discussed in terms of electrical, spectroscopies and surface properties. The strengths and weaknesses of these cathodes are outlined, aiming to explain some discrepancies and unclarified issues encountered in the literature. The authors state that this survey can be useful for the future design of high-performance mixed polyanionic cathodes for alkaline-ion rechargeable batteries.

3.3. Prussian Blue analogues as cathode materials

Prussian Blue and its analogues (PBAs) have general composition expressed by the formula Na_xM₂[M₁(CN)₆]_y·nH₂O (x limited between 0 and 2, and y is limited between 0 and 1), where M₁ and M₂ are transition metals from the group Mn, Fe, Co, Cu, Ni etc. They may be easily synthesized by precipitation from the aqueous solution of potassium hexacyanoferrate, upon addition of solutions of Mn Fe Co Ni or Cu salts, and this reaction is well known in analytical chemistry serving to detection of transition metal cations. Most PBAs are cubic phases with 6-fold coordination of MII,III-O₆ octahedra The CN

groups interconnect the ions of transition metals making a basic crystal framework (Figure 8). The space within this tridimensional framework is usually filled with water molecules (zeolitic water), which may be removed by drying.

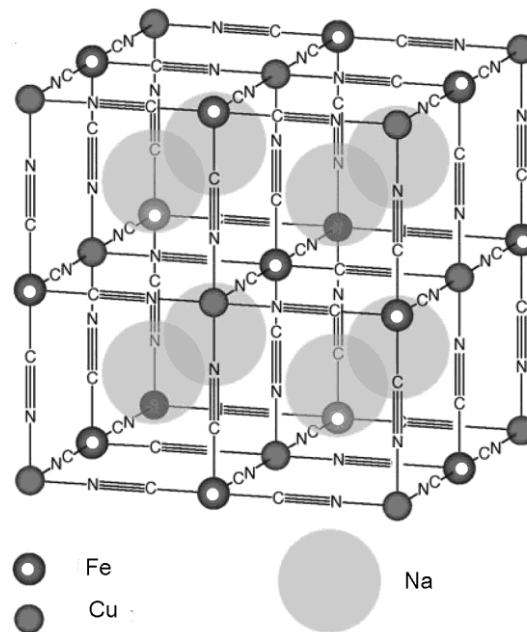


Figure 8. Prussian Blue crystals Na_xCu[FeCN]₆,
The three-dimensional diffusion of Na ions is allowed through the solid network

The ability of PBAs to intercalate reversibly alkaline cations is known for a long time. Wessels et al [47,48] synthesized copper and mixed copper/nickel hexacyanoferrates and reported that they intercalate Na⁺ ions in an aqueous solution at less than 2 V against a standard hydrogen electrode. With a negative polarization, sodium ions insert into the free sites within three-dimensional Na⁺ migration pathways. Low diffusion energy barriers for sodium ions enable fast diffusion of 3D type, and consequently, fast intercalation/deintercalation reactions. The modifications of chemical compositions by insertion or deinsertion of alkaline cations do not influence the overall crystalline structure. In the aqueous solutions studied, the long cycle life of even 2000 cycles at a rate of 500 mA g⁻¹ was reported for both copper and mixed copper-nickel hexacyanoferrates.

Lu et al [49] studied Na_xMFe[CN]₆ (M: Fe and Mn) in an organic electrolyte solution, which exhibited high operation voltage plateaus at 3.8 V for charge and 3.5 V for discharge. In an extended study, the concentration of Na in the Na_xMFe[CN]₆ varied from Na_{1.4}MFe[CN]₆ to Na_{1.72}MFe[CN]₆.

The structure of this compound displayed high stability suffering no change after 50 charging/discharging cycles.

$\text{Na}_{1.72}\text{MFe}[\text{CN}]_6$ displayed appreciable capacity at a high charging/discharging rate of 40C. Replacement of Mn with Fe, in $\text{Na}_x\text{MnFe}[\text{CN}]_6$, lowered the operation voltage of the lower voltage plateau to 3.1 V on charge and 2.8 V on discharge, delivering a discharge capacity of approximately 120 mAh g^{-1} . The electrode kept a stable capacity over 600 cycles.

You et al [50] synthesized Na-enriched Prussian blue, $\text{Na}_{1+x}\text{Fe}^{\text{III}}[\text{Fe}^{\text{II}}(\text{CN})_6]$ from the solution of ferric salt which was added under stirring to a solution of $\text{Na}_4\text{Fe}(\text{CN})_6$. They take particular care to minimize the number of crystal vacancies consisting in absence of $\text{Fe}(\text{CN})_6$ units, which are formed readily under circumstances of forced precipitation. Namely, these vacancies are occupied by structural water, the removal of which may deteriorate intercalation capacity, or even bring to the collapse of the complete structure. Another type of water, the zeolitic one also exists in these compounds, occupying the sites necessary for sodium-ion intercalation. Therefore, this type of water should be eliminated as much as possible. Using well crystallized,

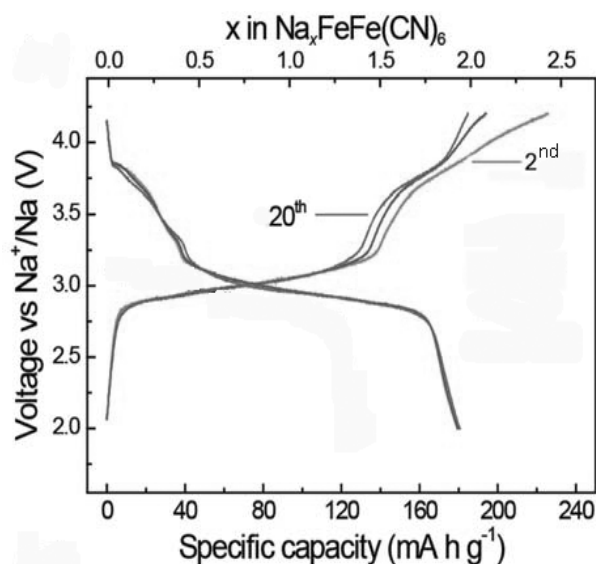


Figure 9. Galvanostatic charging/discharging curve (2nd - 20th cycle) of $\text{Na}_x\text{Fe}[\text{Fe}(\text{CN})_6]$ in 1 M NaPF_6 in EC and DEC (1:1 volume ratio) [49]
Copyright: The Royal Society of Chemistry 2014

almost structural water-free samples, the authors studied the electrochemical behavior in an electrolyte solution composed of 1 M NaPF_6 dissolved in ethylene carbonate (EC) and diethyl carbonate (DEC) at a 1:1 volume ratio. They found a high specific capacity of 170 mAh g^{-1} , with the mean voltage close to 3 V versus metallic sodium, without apparent capacity loss after 150 cycles (Figure 9). For full capacity utilization, both ferrous and ferric ions, participate in the redox reactions accompanying intercalation /de-intercalation processes, to maintain the electro-neutrality of the solid phase.

Li et al [51] synthesized Na-enriched $\text{Na}_{1+x}\text{FeFe}(\text{CN})_6$ starting with the $\text{Na}_4\text{Fe}(\text{CN})_6$ as the precursor in NaCl solutions. The electrochemical results of 1.0 mol/L NaClO_4 in ethylene carbonate (EC)–diethyl carbonate solution (1:1 v/v) for $\text{Na}_{1.56}\text{Fe}[\text{Fe}(\text{CN})_6] \cdot 3.1\text{H}_2\text{O}$ sample show a high specific capacity of more than 100 mAh g^{-1} and excellent capacity retention of 97% over 400 cycles. The authors claimed they found a promising cathode for sodium-ion batteries.

Xiao et al. [52] studied the changes in the structure of $\text{Na}_2\text{FeMn}(\text{CN})_6$ cathode upon sodium intercalation. They concluded that a maximum of two Na^+ ions per formula unit may be incorporated if both the M1 and the M2 transition metal elements may accommodate their oxidation state leading to a theoretical specific capacity of 170 mAh g^{-1} . This was proven experimentally by Shen et al [53] Namely, these authors synthesized sodium manganese hexacyanoferrate $\text{Na}_x\text{MnFe}(\text{CN})_6$ as a solid precipitate, starting with the aqueous solution of sodium hexacyanoferrate ($\text{Na}_4\text{Fe}(\text{CN})_6 \cdot 10\text{H}_2\text{O}$), manganese sulfate monohydrate ($\text{MnSO}_4 \cdot \text{H}_2\text{O}$), sodium chloride (NaCl) and sodium citrate dehydrate ($\text{Na}_3\text{C}_6\text{H}_5\text{O}_7 \cdot 2\text{H}_2\text{O}$). The solid precipitate was separated and dried. In galvanostatic charging/discharging experiments, the product displayed an almost flat galvanostatic charging/discharging plateau at a mean voltage of 3.6 V vs sodium metal. The galvanostatic charging/discharging curves indicated a large coulombic capacity of 144 mAh g^{-1} under a 0.1 C rate, good rate performance (115.6 mAh g^{-1} under a 1 C rate, 86.6 mAh g^{-1} under a 10 C rate), and good cycling stability (73.4% retention after 780 cycles under a 0.5 C rate, and 72.7% retention after 2100 cycles under a 1 C rate).

4. Na-ION BATTERIES WITH SOLID ELECTROLYTE (ALL-SOLID-STATE Na-ION BATTERIES)

All-solid-state sodium batteries (ASSSBs) attract nowadays considerable attention being nonflammable, and thus much safer than Li-ion batteries. Their performance depends on the conductivity of the solid electrolyte and the quality and durability of the contact on the electrode-electrolyte interface. Hayashi et al [54] investigated sulfide-based solid electrolyte, Na_3PS_4 with mobile Na ions. For the synthesis, they used the mixture of 75 mol % of Na_2S and 25 mol % of P_2S_5 (mol%), which by ball milling, for 1.5 h was transformed into Na_3PS_4 crystals. After heat treatment at 270 °C for 1 h, this glass-ceramic electrolyte displayed the highest conductivity of $4.6 \times 10^{-4} \text{ S cm}^{-1}$. Then they constructed an all-solid-state battery with Na_xSn anode and NaCrO_2 cathode. This battery displayed a specific capacity of 60 mAh g^{-1} (calculated on a NaCrO_2 basis) during 15 cycles. The short cycle life of this battery is caused by the problems with the electrode/electrolyte interface. Namely, during Na ion intercalation, the cathode swells in size and shrinks during Na ion deintercalation. The repeated swelling and shrinking lead to the cracking of brittle ceramic electrolyte and caused its detachment from the solid electrolyte, which shortens the battery cycle life. To mitigate this problem, Yao et al [55] from the University of Houston in Texas, created a flexible organic cathode, consisting of pyrene-4,5,9,10-tetraone (PTO) and 10 % carbon black additive. This material displayed an initial specific capacity of 314 mAh g^{-1} and enabled the composition of a battery with $\text{Na}_{15}\text{Sn}_4$ alloy displaying a high energy

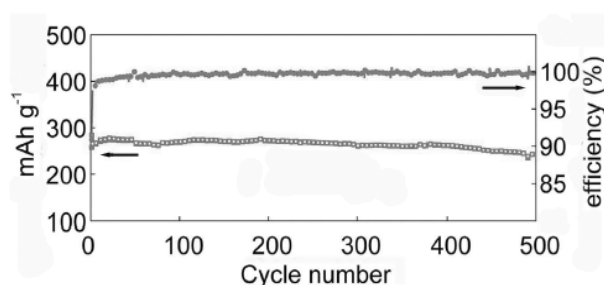


Figure 10. Specific capacity and coulombic efficiency in function of Cycle number for all solid-state battery PTO(C)/ Na_3PS_4 / $\text{Na}_{15}\text{Sn}_4$ at rate 0.01 C at temperature 60 °C (55)

density of 587 Wh kg^{-1} , close to actual lithium-ion cells. The flexibility of organic material enabled long cycle life. Namely, after 500 charge and discharge cycles at a rate of 0.01 C at a temperature of 60 °C, the capacity retains 89% of its initial value, which is a similar performance to conventional lithium-ion cells. The voltage of the cell is below that causing the decomposition of electrolyte, which additionally supports long cycle life.

5. PRODUCTION OF FIRST GENERATION OF Na-ION BATTERIES

A couple of companies already started commercial production of Na-ion batteries.

Natron Energy in Santa Clara, California, produces both the cathode and anode from Prussian Blue, (transition metal hexacyanoferrates). The chemical structure of these materials enables easy three-dimensional diffusion of sodium ions, and the battery can be charged and discharged in minutes. Battery with Prussian Blue electrodes can withstand more than 50,000 charging cycles. Nowadays, Natron's customers are data centers and telecom companies. In September 2020, the Department of Energy's Advanced Research Projects Agency-Energy awarded – Norton with USD 19.9 million as part of a new program to advance its commercialization efforts, since the batteries are now in low-volume production [56].

The other leading sodium-ion battery company is the British company Faradion [57,58]. This company uses their type of hard carbon anode, and several types of cathodes – layered, polyphosphate etc. They announced cooperation with investment group ICM Australia since the demand for residential, commercial and grid scale applications batteries in Australia is growing. They also develop batteries for commercial vehicles in India.

Currently, Faradion prototype cells can deliver an energy density of over 140 Wh kg^{-1} . The company announced cooperation with the energy company Phillips 66 from Houston in the development of lower-cost and higher-performing anode materials and plans the cooperation with Pacific Northwest National Laboratory from the USA, the French National Center for Scientific Research (CNRS), and the French research network on electrochemical energy storage, among

others, to attain practical energy of Na-ion batteries of nearly 200 Wh kg⁻¹. [58]

Famous Chinese battery supplier CATL declared the production of sodium-ion batteries [59]. The cathode material is Prussian White modified to avoid rapid capacity fading during cycling. The anode is porous hard carbon. The battery can charge fast, namely, it may be charged



Figure 11. CATLs prismatic and cylindrical Na-ion Battery cell versions [59]

to 80% in 15 minutes at room temperature. It is also less sensitive to temperature changes than a conventional Li-ion battery. The initial version displays an energy density of 160 Wh kg⁻¹, however, the next generation, which is currently under development, is expected to offer an energy density of 200 Wh kg⁻¹.

Among others, one may still mention AGM Batteries Ltd established in 1997 in Thurso, Caithness, NGK Insulators Ltd, established in 1919 in Nagoya, Japan, HiNa Battery Technology Co. Ltd, established in 2007 in Zhongguancun, Liyang Tiamat Energy, established in 2017 (founder Laurent Hubard) and Altris, established in 2017 in Uppsala, Sweden.

In Table 1 the comparison is made of the main (available) characteristics of actual Li-ion batteries to commercial Na-ion batteries of the first generation produced by some battery providers.

Table 1. Comparison of available characteristics of the first generation of commercial Na-ion batteries to the ones of contemporary Li-ion cells in a form of standard 18650 cylindrical cells (18 mm in diameter, 65 mm in length)

18650 cells	Voltage	Wh kg ⁻¹	Wh L ⁻¹	Cycle life
graphite(C)/LiCoO ₂ - (Li-ion)	3.7	206	530	
C/LiNi _{0.33} Mn _{0.33} Co _{0.33} O ₂ - (Li-ion)	3.6	210	530	
C/LiNi _{0.8} Co _{0.15} Al _{0.05} O ₂ - (Li-ion)	3.6	285	785	
C/LiFePO ₄ - (Li-ion)	3.4	126	325	
Farradion hard carbon/unknown cathode (Na-ion)		140		
CNRS CEA - (Na-ion) (ref [60])		90	250	2000
PNNL-WSU NaNi _{0.68} Mn _{0.22} Co _{0.10} O ₂ -hard carbon (Na-ion) (ref [61])	2.7	150	375	
ALISTORE hard carbon/Na ₃ V ₂ (PO ₄) ₂ F ₃) (ref [62])	3.5	75		4000 cycles (1 C rate)
CATL hard carbon/Prussian White (ref [59])		160		

6. CONCLUSION

Lithium-ion batteries serve today as energy sources for portable electronics and electric cars. Thanks to their high energy density which attains roughly Wh kg⁻¹. Their non-sustainability arises from the use in their production of elements being deficient in the earth's crust (lithium, cobalt, nickel). As a response to an exponentially growing demand for batteries on the world market, from 2010-ties, the researchers invest much effort in the development of more sustainable batteries, and the

solutions are seen in sodium-ion batteries. During the last decade, several companies developed the first generation of sodium-ion batteries for commercial purposes. The advantage of their production is the consumption of elements very abundant in the earth's crust.

Their disadvantage is the relatively low energy density of 70-160 Wh kg⁻¹ thus they are uncompetitive in the battery market, although they may as such already be used for low-demanding purposes, such as grid voltage stabilization. A rapid advance in the development of sodium-ion

batteries, reviewed in this article, with the anode materials approaching 500 Wh kg⁻¹ and cathode materials approaching the capacity of 200 Wh kg⁻¹, offers the promise of achieving from Na-ion batteries of the second generation a high level of competitiveness to the Li-ion batteries. This hope is supported by the fact that the duration of the development of Na-ion batteries is only one-third of the duration of the development of Li-ion batteries.

7. ACKNOWLEDGEMENT

This work is supported by the Ministry of Education, Science and Technological Development of the Republic of Serbia (contract No. 451-03-9/2021-14/200146) and by the Serbian Academy of Sciences and Arts through the project F-190: Electrocatalysis in Contemporary Processes of Energy Conversion.

8. REFERENCES

- [1] C. Pillot, *The Rechargeable Battery Market and Main Trends 2016-2025*; The International Battery Seminar and Exhibit Virtual Conference, Lisbon Portugal, September 20, 2017; https://rechargebatteries.org/wp-content/uploads/2020/01/avicenne-energy_pillot-2017.pdf [accessed: 30 June 2020].
- [2] K. Turcheniuk, D. Bondarev, V. Singhal, G. Yushin, *Ten years left to redesign lithium-ion batteries*, *Nature*, Vol. 559 (2018) 467–470.
- [3] S. Mentus, *The role of batteries in near future energetics*, *Contemporary Materials*, Vol. XII-1 (2021) 1–15.
- [4] K. M. Abraham, *How Comparable Are Sodium-Ion Batteries to Lithium-Ion Counterparts?*, *ACS Energy Lett.*, Vol. 5 (2020) 3544–3547.
- [5] M. D. Slater, D. Kim, E. Lee, C. S. Johnson, *Sodium-Ion Batteries*, *Adv. Funct. Mater.*, Vol. 23 (2013) 947–958.
- [6] P. Ge, M. Foulletier, *Electrochemical interaction of sodium in graphite*, *Solid State Ionics*, Vol. 28–30 (1988) 1172–1175.
- [7] D. P. Divincenzo, E. J. Mele, *Cohesion and structure in stage-1 graphite intercalation compounds*, *Phys. Rev. B*, Vol. 32 (1985) 2538–2553.
- [8] D. A. Stevens, J. R. Dahn, *High capacity anode material for rechargeable sodium-ion batteries*, *J. Electrochem. Soc.*, Vol. 147 (2000) 1271–1273.
- [9] S. Wenzel, T. Hara, J. Janek, P. Adelhelm, *Room-temperature sodium-ion batteries: Improving the rate capability of carbon anode materials by templating strategies*, *Energy Environ. Sci.*, Vol. 4 (2011) 3342–3345.
- [10] X. Zhou, Y. G. Guo, *Highly disordered carbon as a superior anode material for room temperature sodium-ion batteries*, *ChemElectrochem*, Vol. 1 (2014) 83–86.
- [11] P. C. Tsai, S. C. Chung, S. K. Lin, A. Yamada, *Ab initio study of sodium intercalation into disordered carbon*, *J. Mater. Chem. A*, Vol. 3 (2015) 9763–9768.
- [12] C. Bommier, T. W. Surta, M. Dolgos, X. Ji, *New mechanistic insights on Na-ion storage in nongraphitizable carbon*, *Nano Lett.*, Vol. 15 (2015) 5888–5892.
- [13] R. M. N. M. Rathnayake, T. T. Duignan, D. J. Searles, X. S. Zhao, *Exploring the effect of interlayer distance of expanded graphite for sodium ion storage using first principles calculations*, *Physical Chemistry Chemical Physics*, Vol. 23 (2021) 3063–3070.
- [14] J. Y. Hwang, S. T. Myung, Y. K. Sun, *Sodium-ion batteries: present and future*, *ChemSocRev*, Vol. 46 (2017) 3485–3856.
- [15] S. Wang, L. Xia, L. Yu, L. Zhang, H. Wang, X. W. D. Lou, *Free-Standing Nitrogen-Doped Carbon Nanofiber Films: Integrated Electrodes for Sodium-Ion Batteries with Ultralong Cycle Life and Superior Rate Capability*, *Adv. Energy Mater.*, Vol. 6 (2016) 1502217.
- [16] W. Li, M. Zhou, H. Li, K. Wang, S. Cheng, K. Jiang, *A high performance sulfur-doped disordered carbon anode for sodium ion batteries*, *Energy Environ. Sci.*, Vol. 8 (2015) 2916–2921.
- [17] Y. Li, L. Zhang, X. Wang, X. Xia, D. Xie, C. Gu, J. Tu, *Sodium storage behavior of electron-rich element-doped amorphous carbon*, *Appl. Phys. Rev*, Vol. 8 (2021) 11402.
- [18] Y. Wen, K. He, Y. Zhu, F. Han, Y. Xu, I. Matsuda, Y. Ishii, J. Cumings, C. Wang, *Expanded graphite as superior anode for sodium-ion batteries*, *Nat Commun*, Vol. 5 (2014) 4033.
- [19] Y. X. Wang, S. L. Chou, H. K. Liu, S. X. Dou, *Reduced graphene oxide with superior cycling stability and rate capability for sodium storage*, *Carbon*, Vol. 57 (2013) 202–208.

- [20] J. Ding, H. Wang, Z. Li, A. Kohandehghan, K. Cui, Z. Xu, B. Zahiri, X. Tan, E. M. Lotfabad, B. C. Olsen, D. Mitlin, *Carbon nanosheet frameworks derived from peat moss as high performance sodium ion battery anodes*, *ACS Nano*, Vol. 7 (2013) 11004–11015.
- [21] A. S. Dobrota, I. A. Pašti, S. V. Mentus, B. Johansson, N. V. Skorodumova, *Functionalized graphene for sodium battery applications: the DFT insights*, *Electrochimica Acta*, Vol. 250 (2017) 185–195.
- [22] L. David, R. Bhandavat, G. Singh, *MoS₂/Graphene Composite Paper for Sodium-Ion Battery Electrodes*, *ACS Nano*, Vol. 8 (2014) 1759–1770.
- [23] Q. Pan, Q. Zhang, F. Zheng, Y. Liu, Y. Li, X. Ou, X. Xiong, C. Yang, M. Liu, *Construction of MoS₂/C Hierarchical Tubular Heterostructures for High-Performance Sodium Ion Batteries*, *ACS Nano*, Vol. 12–12 (2018) 12578–12586.
- [24] Y. Jiang, D. Song, J. Wu, Z. Wang, S. Huang, Y. Xu, Z. Chen, B. Zhao, J. Zhang, *Sandwich-like SnS₂/Graphene/SnS₂ with Expanded Interlayer Distance as High-Rate Lithium/Sodium-Ion Battery Anode Materials*, *ACS Nano*, Vol. 13–8 (2019) 9100–9111.
- [25] X. Ou, L. Cao, X. Liang, F. Zheng, H. S. Zheng, X. Yang, J. H. Wang, C. Yang, M. Liu, *Fabrication of SnS₂/Mn₂SnS₄/Carbon Heterostructures for Sodium-Ion Batteries with High Initial Coulombic Efficiency and Cycling Stability*, *ACS Nano*, Vol. 13 (2019) 3666–3676.
- [26] T. Ramireddy, T. Xing, M. M. Rahman, Y. Chen, Q. Dutercq, D. Gunzelmann, A. M. Glushenkov, *Phosphorus–carbon nanocomposite anodes for lithium-ion and sodium-ion batteries*, *J. Mater. Chem. A*, Vol. 3 (2015) 5572–5584.
- [27] J. Sun, H. W. Lee, M. Pasta, H. Yuan, G. Zheng, Y. Sun, Y. Li, Y. Cui, *A phosphorene-graphene hybrid material as a high-capacity anode for sodium-ion batteries*, *Nat. Nanotechnol.*, Vol. 10 (2015) 980–985.
- [28] A. Abouimrane, W. Weng, H. Eltayeb, Y. Cui, J. Niklas, O. Poluektov, K. Amine, *Sodium insertion in carboxylate based materials and their application in 3.6 V full sodium cells*, *Energy Environ. Sci.*, Vol. 5 (2012) 9632–9638.
- [29] S. Wang, L. Wang, Z. Zhu, Z. Hu, Q. Zhao, J. Chen, *All organic sodium-ion batteries with Na₄C₈H₂O₆*, *Angew. Chem., Int. Ed.*, Vol. 53 (2014) 5892–5896.
- [30] W. Deng, X. Liang, X. Wu, J. Qian, Y. Cao, X. Ai, J. Feng, H. Yang, *A low cost, all-organic Na-ion Battery Based on Polymeric Cathode and Anode*, *Sci Rep*, Vol. 3 (2013) 2671.
- [31] X. Chi, Y. Liang, F. Hao, Y. Zhang, J. Whiteley, H. Dong, P. Hu, S. Lee, Y. Yao, *Tailored organic electrode material compatible with sulfide electrolyte for stable all-solid-state sodium batteries*, *Angew. Chem. Int. Ed.*, Vol. 57–10 (2018) 2630–2634.
- [32] B. Ma, Y. Lee, P. Bai, *Dynamic Interfacial Stability Confirmed by Microscopic Optical Operando Experiments Enables High-Retention-Rate Anode-Free Na Metal Full Cells*, *Advanced Science*, Vol. 8 (2021) 2005006.
- [33] X. H. Ma, H. L. Chen, G. Ceder, *Electrochemical Properties of Monoclinic NaMnO₂*, *J. Electrochem. Soc.*, Vol. 158 (2011) A1307–A1312.
- [34] S. Guo, H. Yu, Z. Jian, P. Liu, Y. Zhu, X. Guo, M. Chen, M. Ishida, H. Zhou, *A high-capacity, low-cost layered sodium manganese manganese oxide material as cathode for sodium-ion batteries*, *ChemSusChem*, Vol. 7 (2014) 2115–2119.
- [35] Z. Lu, J. R. Dahn, *In situ X-Ray Diffraction study of P2 Na_{2/3}[Ni_{1/3}Mn_{2/3}]O₂*, *J. Electrochem. Soc.*, Vol. 148 (2001) A1225–A1229.
- [37] D. Kim, M. Cho, K. Cho, *Rational Design of Na(Li_{1/3}Mn_{2/3})O₂ Operated by Anionic Redox Reactions for Advanced Sodium-Ion Batteries*, *Adv. Mater.*, Vol. 29 (2017) 1701788.
- [38] Q. Wang, S. Mariyappan, G. Rousse, A. V. Morozov, B. Porcheron, R. Dedryvère, J. Wu, W. Yang, L. Zhang, M. Chakir, M. Avdeev, M. Deschamps, Y. S. Yu, J. Cabana, M. L. Doublet, A. M. Abakumov, J. M. Tarascon, *Unlocking anionic redox activity in O3-type sodium 3d layered oxides via Li substitution*, *Nat Mater.*, Vol. 20–3 (2021) 353–361.
- [39] F. Sanz, C. Parada, U. Amador, M. A. Monge, C. R. Valero, *Na₄Co₃(PO₄)₂P₂O₇, a New Sodium Cobalt Phosphate Containing a Three-Dimensional System of Large Intersecting Tunnels*, *J. Solid. State Chem.*, Vol. 123–1 (1996) 129–139.
- [40] H. Kim, I. Park, D. H. Seo, S. Lee, S. W. Kim, W. J. Kwon, Y. U. Park, C. S. Kim, S. Jeon, K. Kang, *New iron-based mixed-polyanion cathodes for lithium and sodium rechargeable batteries: combined first principles calculations and experimental study*, *J. Am. Chem. Soc.*, Vol. 134 (2012) 10369–10372.
- [41] H. Kim, I. Park, S. Lee, H. Kim, K. Y. Park, Y. U. Park, H. Kim, J. Kim, H. D. Lim, W. S.

Yoon, K. Kang, *Understanding the Electrochemical Mechanism of the New Iron-Based Mixed-Phosphate $\text{Na}_4\text{Fe}_3(\text{PO}_4)_2(\text{P}_2\text{O}_7)$ in a Na Rechargeable Battery*, Chem. Mater., Vol. 25 (2013) 3614–3622.

[42] M. Nose, H. Nakayama, K. Nobuhara, H. Yamaguchi, S. Nakanishi, H. Iba, *$\text{Na}_4\text{Co}_3(\text{PO}_4)_2\text{P}_2\text{O}_7$: A novel storage material for sodium-ion batteries*, J. Power Sources, Vol. 234 (2013) 175–179.

[43] S. Y. Lim, H. Kim, J. Chung, J. H. Lee, B. G. Kim, J. J. Choi, K. Y. Chung, W. Cho, S. J. Kim, W. A. Goddard III, Y. Jung, J. W. Choi, *Role of intermediate phase for stable cycling of $\text{Na}_7\text{V}_4(\text{P}_2\text{O}_7)_4\text{PO}_4$ in sodium ion battery*, Proc. Natl. Acad. Sci. U. S. A., Vol. 111–2 (2014) 599–604.

[44] S. Yuvaraj, W. Oh, W. S. Yoon, *Recent progress on sodium vanadium fluorophosphates for high voltage sodium ion battery*, J. Electrochem. Sci. Technol., Vol. 10 (2019) 1–13.

[45] J. Zhao, X. Yang, Y. Yao, Y. Gao, Y. Sui, B. Zou, H. Ehrenberg, G. Chen, F. Du, *Moving to Aqueous Binder: A Valid Approach to Achieving High-Rate Capability and Long-Term Durability for Sodium-Ion Battery*, Adv. Sci., Vol. 5–4 (2018) 1700768.

[46] A. Gezović, M. Vujković, M. Milović, V. Grudić, R. Dominko, S. Mentus, *Recent developments of $\text{Na}_4\text{M}_3(\text{PO}_4)_2(\text{P}_2\text{O}_7)$ as the cathode material for alkaline-ion rechargeable batteries: challenges and outlook*, Energy Storage Materials, Vol. 37 (2021) 243–273.

[47] C. D. Wessells, M. T. McDowell, S. V. Peddada, M. Pasta, R. A. Huggins, Y. Cui, *Tunable reaction potentials in open framework nanoparticle battery electrodes for grid-scale energy storage*, ACS Nano, Vol. 6–2 (2012) 1688–1694.

[48] C. D. Wessells, S. V. Peddada, M. T. McDowell, R. A. Huggins, Y. Cui, *The Effect of Insertion Species on Nanostructured Open Framework Hexacyanoferrate Battery Electrodes*, J. Electrochem. Soc., Vol. 159–2 (2012) A98–A103.

[49] Y. H. Lu, L. Wang, J. G. Cheng and J. B. Goodenough, *Prussian blue: a new framework of electrode materials for sodium batteries*, Chem. Commun., Vol. 48 (2012) 6544–6546.

[50] Y. You, X. L. Wu, Y. X. Yin, Y. G. Guo, *High-quality Prussian blue crystals as superior cathode materials for room-temperature sodium-ion batteries*, Energy Environ. Sci., Vol. 7 (2014) 1643–1647.

[51] W. J. Li, S. L. Chou, J. Z. Wang, Y. M. Kang, J. L. Wang, Y. Liu, Q. F. Gu, H. K. Liu, S. X. Dou, *Facile method to synthesize Na-enriched $\text{Na}_{1+x}\text{FeFe}(\text{CN})_6$ frameworks as cathode with superior electrochemical performance for sodium-ion batteries*, Chem. Mater., Vol. 27 (2015) 1997–2003.

[52] P. Xiao, J. Song, L. Wang, J. B. Goodenough, G. Henkelman, *Theoretical Study of the Structural Evolution of a $\text{Na}_2\text{FeMn}(\text{CN})_6$ Cathode upon Na Intercalation*, Chem. Mater., Vol. 27 (2015) 3763–3768.

[53] Z. Shen, S. Guo, C. Liu, Y. Sun, Z. Chen, J. Tu et al., *Na-rich Prussian white cathodes for long-life sodium-ion batteries*. ACS Sustain. Chem. Eng. 6 (2018) 16121–16129.

[54] A. Hayashi, K. Noi, N. Tanibata, M. Nagao, M. Tatsumisago, *High sodium ion conductivity of glass/ceramic electrolytes with cubic Na_3PS_4* , J Power Sources, Vol. 258 (2014) 420–423.

[55] F. Hao, X. Chi, Y. Liang, K. Zhao, J. Lou, Y. Yao, *Taming Active Material-Solid Electrolyte Interfaces with Organic Cathode for All-Solid-State Batteries*, Joule, Vol. 3–5 (2019) 1349–1359.

[56] <https://natron.energy/news-and-events/> [accessed: 18 July 2021].

[57] K. M. Abraham, *How Comparable Are Sodium-Ion Batteries to Lithium-Ion Counterparts?*, ACS Energy Lett., Vol. 5 (2020) 3544–3547.

[58] Phillips 66 and Faradion Developing Sodium-ion Battery Materials | Business Wire <https://investor.phillips66.com/financial-information/news-releases/news-release-details/2021/Phillips-66-and-Faradion-Developing-Sodium-ion-Battery-Materials/default.aspx> [accessed: 25 September 2021].

[59] https://www.greencarreports.com/news/1133059_first-catl-sodium-ion-batteries-revealed-can-charge-to-80-in-15-minutes [accessed: 14 September 2021]

[60] <https://news.cnrs.fr/articles/a-battery-revolution-in-motion> [accessed: 20 March 2021]

[61] J. Song, K. Wang, J. Zheng, M. H. Engelhard, B. Xiao, E. Hu, Z. Zhu, C. Wang, M. Sui, Y. Lin, D. Reed, V. L. Sprenkle, P. Yan, X. Li, *Controlling Surface Phase Transition and Chemical Reactivity of O₃-Layered Metal Oxide Cathodes for High-Performance Na-Ion Batteries*, ACS Energy Lett. Vol. 5–6 (2020) 1718–1725.

- [62] T. Broux, F. Fauth, N. Hall, Y. Chatillon, M. Bianchini, T. Bamine, J. B. Leriche, E. Suard, D. Carlier, Y. Reynier, L. Simonin, C. Masquelier, C. L. Croguennec, *High Rate Performance for Carbon-coated $\text{Na}_3\text{V}_2(\text{PO}_4)_2\text{F}_3$ in Na-ion Batteries*, *Small Methods*, Vol. 3–4 (2019) 1800215–1800237.

НОВОСТИ У РАЗВОЈУ НАТРИЈУМ-ЈОНСКИХ БАТЕРИЈА

Сажетак: Данас литијум-јонске батерије доминирају као извори енергије за преносиве електронске уређаје (мобилне телефоне, лаптоп рачунаре) као и за електричне аутомобиле. Главни проблем који се тиче њихове употребе је ограничена одрживост: сировине за њихову производњу, литијум, кобалт и никл дефицитарни су у Земљиној кори. Потенцијално исцрпљивање рударских ресурса прети да заустави производњу. С друге стране, натријум-јонске батерије, које раде на сличним принципима као и литијум-јонске батерије, представљају праву одрживу алтернативу. Наиме, количина натријума у Земљиној кори далеко је већа у поређењу са литијумом, а надаље, натријум-јонске батерије могу се производити и са веома заступљеним металима, без кобалта и никла. Стога је развој натријум-јонских батерија предмет интересовања великог броја истраживачких група широм света. Тренутно је главни недостатак натријум-јонских батерија у односу на литијум-јонске батерије нижа густина енергије (~ 50%), па је њихова конкурентност на тржишту и даље релативно ниска и обезбеђује за сада само комплементарне видове коришћења, у мање захтевним областима (као што је стабилизација мрежног напона). Међутим, недавно су остварена бројна побољшања што обећава брзо повећање конкурентности натријум-јонских батерија у својим подручјима употребе. У овом раду дат је преглед најновијег напретка постигнутог у побољшању материјала аноде и катоде, који омогућава високе електрохемијске перформансе натријум-јонских батерија. Такође, направљен је преглед својстава комерцијалних верзија батерија прве генерације доступан у литератури.

Кључне речи: натријум-јонске батерије, катодни материјали, анодни материјали, комерцијалне верзије батерија.

Paper received: 9 August 2021

Paper accepted: 16 February 2022
